View metadata, citation and similar papers at core.ac.uk
brought to you by CORE
provided by CiteSeerX

GEOPHYSICAL RESEARCH LETTERS, VOL. 29, NO. 0, 10.1029/2000GL011447, 2002

Heterogeneous reactions in aircraft gas turbine engines

R. C. Brown and R. C. Miake-Lye
Aerodyne Research, Inc., Billerica, MA, USA

S. P. Lukachko and I. A. Waitz
Massachusetts Institute of Technology, Cambridge, MA, USA

Received 11 January 2000; revised 7 March 2002; accepted 10 April 2002; published XX Month 2002.

[1] One-dimensional flow models and unity probability heterogeneous rate parameters are used to estimate the maximum effect of heterogeneous reactions on trace species evolution in aircraft gas turbines. The analysis includes reactions on soot particulates and turbine/nozzle material surfaces. Results for a representative advanced subsonic engine indicate the net change in reactant mixing ratios due to heterogeneous reactions is $<10^{-6}$ for O_2, CO_2, and H_2O, and $<10^{-10}$ for minor combustion products such as SO_2 and NO_2. The change in the mixing ratios relative to the initial values is <0.01%. Since these estimates are based on heterogeneous reaction probabilities of unity, the actual changes will be even lower. Thus, heterogeneous chemistry within the engine cannot explain the high conversion of SO_2 to SO_3 whicsome wake models require to explain the observed levels of vola tile aerosols. Furthermore, turbine heterogeneous processes will not effect exhaust NO_x or NO_y levels. *INDEX TERMS:* 0305 Atmospheric Composition and Structure: Aerosols and particles (0345, 4801); 0317 Atmospheric Composition and Structure: Chemical kinetic and photochemical properties; 0399 Atmospheric Composition and Structure: General or miscellaneous

1. Introduction

[2] Trace species emissions from gas turbine engines are of interest because of environmental and human health considerations. While combustion, air quality, and atmospheric change research have significantly enhanced our understanding of the relevant chemistry, the list of emissions that are considered pollutants has expanded, and acceptable emission levels have been lowered. It is thus expected that the challenges faced by engine design engineers will continue to evolve, with emission requirements growing more stringent. Developing technologies to meet these challenges will increase the demands placed on our ability to characterize the chemical kinetic and fluid dynamical mechanisms governing trace species chemistry in the engine. New diagnostic techniques and more robust and accurate numerical modeling capabilities for realistic combustor and turbine geometries will be required.

[3] A numerical model, CNEWT, was recently developed to describe trace species evolution in gas turbine engines [*Lukachko*, 1997; *Lukachko et al.*, 1998]. CNEWT bridges the gap between detailed fluid dynamical without chemistry and detailed chemistry neglecting fluid dynamical effects. CNEWT was initially used to explore gas phase chemistry in an aircraft gas turbine engine [*Lukachko et al.*, 1998] associated with gas phase precursors (SO_3, H_2SO_4, HNO_3) to volatile aerosol formation in the aircraft wakes.

[4] As further evaluation of the impact of engine fluid dynamics continues, investigations of additional effects on trace species evolution are needed. One unexplored issue is the impact of heterogeneous reaction kinetics. Evaluating heterogeneous reactions through detailed modeling of the coupled fluid dynamics and chemistry is a costly procedure. Thus, a first order identification of the trace species whose emission levels might be influenced by heterogeneous kinetics in the turbine flow would be useful.

[5] The focus of this paper is the use of simple one-dimensional kinetic models to estimate upper limits for the expected impact of heterogeneous reactions and to ascertain the need for more detailed analysis for specific gas phase reactants. Section 2 describes the advanced subsonic engine selected for study and the methodology developed to specify the near-wall flows along the gas path. Results for heterogeneous reactions on soot particulates are given in Section 3. Results for reactions on turbine surfaces are given in Section 4. The conclusions reached based on this analysis and discussions of the primary uncertainties are given in Section 5.

2. Near-Wall Interactions

[6] Results are reported for a conceptual, advanced subsonic engine (ASE) that is projected to enter service in 2005. The ASE, developed by the NASA Glenn Research Center [*Liebeck et al.*, 1995], is a two-spool turbofan with a bypass ratio of 11, an overall pressure ratio of 45, a combustor exit total temperature of 1611 K, and a Mach 0.8 thrust of 30.3 kN at an 11 km cruise altitude. This parameter range is reasonably consistent with modern engines and the ASE can be considered representative of both current and near future engines.

[7] Internal surface areas were approximated based on the gas path geometry and assumed blade geometries. Total surface areas of 5.7 m^2 for the endwalls and 6.8 m^2 for the blades were calculated for an internal surface area along the combustor exit to nozzle exit gas path of 12.5 m^2. Using a nominal spherical soot particle radius of 0.065 microns and a uniform particle density of $1.0E^{+07}$ per cm^3, the total soot surface area is approximately 0.122 m^2 and the ratio of engine internal surface area to soot surface area is approximately 100.

[8] An approximate model was developed to estimate the likelihood that a fluid parcel will interact with wall surfaces. Detailed blade-row-by-blade-row flow specifications for average temperature, pressure, velocity, cooling flow, and gas path geometry were used to determine a one-dimensional, two-stream representation with a freestream flow and a near-wall flow. Figure 1 defines the near-wall zone for cross-sections along the post-combustor flow.

[9] In the context of this assessment, the likelihood of wall interaction is determined by three parameters: the surface availability, the extent of the near-wall zone, and mixing within the near-wall zone. Results for a worst-case flow scenario from the perspective of heterogeneous conversion on the wall, for which the availability of the surface is high and the residence time and mixing in the near-wall layer are maximized, are presented below.

[10] The surface availability (a) describes the fraction (S_{avail}) of the total internal surface area (S_{int}) that can interact with combustion gases ($S_{avail} = aS_{int}$). This differs from a surface reactivity in

Copyright 2002 by the American Geophysical Union.
0094-8276/02/2000GL011447$05.00

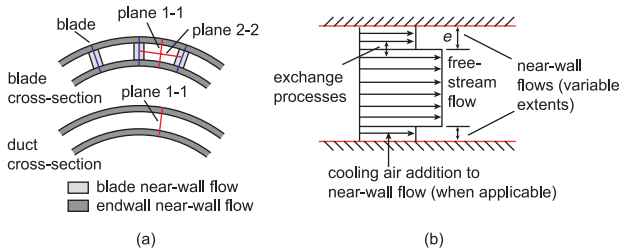

Figure 1. Definition of wall interaction model — (a) engine sector axial view, (b) plane 1–1/2–2 detail.

that the effective surface area available for interaction is determined by flow conditions rather than material properties (*e.g.* film cooling). The factor (a) was set to 1.0 in all sections of the engine except the high-pressure turbine (HPT) where film cooling is active for the engines considered. The effectiveness of this fluid barrier was determined based on the ability of the film cooling coverage to protect the surface from hot freestream gases. Assuming a minimum film cooling effectiveness, $\eta_{ad} = (T_{aw} - T_w)/(T_{aw} - T_c)$, of 0.2 and assuming turbulent Schmidt (Sc_T) and Prandtl (Pr_T) numbers of 1, the factor a was set at 1-η_{ad}, or 0.8. Cooling flow is added within the HPT in a manner specified by the cycle and represents a significant dilution to the near-wall flow, accounting for approximately 25% of the total core flow after the HPT.

[11] The extent of the near-wall zone, specified as a fraction (e) of the hub to casing span or the blade-to-blade pitch from a given surface, determines how much of the engine mass flow is available to react with the wall. This is similar to a boundary layer thickness and represents the extent of wall viscous effects as well as any wall-bounded mixing processes that may bring fluid to the wall. The extent of the near-wall zone is determined primarily from aerodynamic data for turbine and simple shear flows. Measurements and computations of loss, boundary layer growth, blockage, flow angles, velocity, and stagnation quantities were employed [*Brideman et al.*, 1983; *Friedrichs et al.*, 1997; *Hall et al.*, 1998; *Harasgama*, 1990; *Kang et al.*, 1989; *Knight and Choi*, 1989; *Lakshiminarayama*, 1996; *Lakshiminarayama and Govindar*, 1981; *Schlichting*, 1979; *Sharma et al.*, 1988; *Zeschky and Gallus*, 1991]. Values for (e) were specified between 0.05 to 0.25, depending on the reference surface—endwall, blade suction side, or blade pressure side—and whether or not cooling was active.

[12] Surface reactions are driven by mass diffusion and are assumed to occur immediately upon contact with no inefficiency. The near-wall mixing factor (b) determines transport within the near-wall zone through definition of the turbulent diffusion coefficient ($D_t = bD_l$) and thus determines the surface reaction rate. The near-wall flow is assumed to follow the structure of a turbulent boundary layer, with a laminar sub-layer to 1% of the total zone height from the wall and the remaining extent assumed homogeneously turbulent. The laminar sub-layer is specified with binary diffusion coefficients (D_l). Using the turbulent Schmidt number, the laminar diffusion coefficient can be related to the turbulent diffusion coefficient through definition of a mixing factor (b) derived from the comparison of laminar and turbulent viscosities. While the turbulent viscosity should be expected to be variable through the near-wall zone, it is taken to be at least 60–70 times the smallest laminar viscosity ($\nu_t = b\nu_l$, where $b = 60-70$) [*Kuethe and Chow*, 1986].

[13] Exchange between the near-wall and freestream flow zones through the turbine and exhaust nozzle flow, accomplished through turbulent mixing [*Klebanoff*, 1955; *Moss and Oldfield*, 1992; *Shang*, 1995] and viscous layer disturbances (*e.g.* separation, vortical flow), can affect the extent of heterogeneous conversion. This exchange has a finite mixing effectiveness and typically occurs on a time scale slower than that for chemical processes. For example, combustor exit and nozzle exit gaseous emissions measurements indicate that while circumferential variations in species concentrations are small, a basic, radial structure survives through the post combustor flow path [*Lyon and Bahr*, 1981; *Howard et al.*, 1996]. Because the extent of the near-wall layer (e above) is large relative to the overall heterogeneous conversion in the near-wall zone, exchange between the freestream and near-wall layer is not included in the analysis presented.

[14] Temperature and velocity profiles were calculated separately for the freestream and near-wall zones using conservation of mass and energy. Based on typical wall-bounded turbulent flows, it is assumed that the near-wall velocity is at 0.8 times the freestream velocity ($U_{nw} = 0.8U_{free}$). Thus, momentum is not conserved in the transformation from the one-stream to the two-stream flow. The associated error in momentum is less than 2% and represents an uncertainty in the calculated residence time that scales directly with error (*i.e.* ±2%). Density is allowed to vary between the two streams but pressure is assumed to be constant. For the uncooled sections of the gas path, the total temperature of the near-wall and freestream flows are assumed to be the same and equal to the averaged total temperature. Thus, the effects of momentum deficit and secondary flow on the total temperature profile as the gas path is traversed are not accounted. For the cooled sections of the gas path, a wall temperature of 1000 K and an assumption for the near wall to freestream temperature ratio, $(T_{nw} - T_w)/(T_{\text{free}} - T_w)$, was specified. With $Sc_T = 1.0$, the temperature ratio was set equal to the velocity ratio. The resulting near-wall profile with a comparison to the averaged profile is given in Figure 2.

3. Heterogeneous Reactions on Combustion Soot

[15] The number density, size distribution, and composition of exhaust soot particulates depends on the specific engine, power level, and, potentially, altitude. Measurements near the exhaust exit have found mass emission indices ranging between 0.01 and 0.6 g soot/kg-fuel), carbon particle emission indices ranging between 10^{13} and 10^{15} particles/kg-fuel [*Petzold and Schröder*], and mean diameters between 0.05 and 0.08 μm.

[16] Here we report results for two soot size distributions. Distribution 1 is a log-normal distribution (σ = 1.2, r_m = 0.06 μm) that is representative of near field measurements. Distribution 2 is a monodisperse, 10 nm diameter distribution that approximates the soot particles at the turbine inlet assuming negligible agglom-

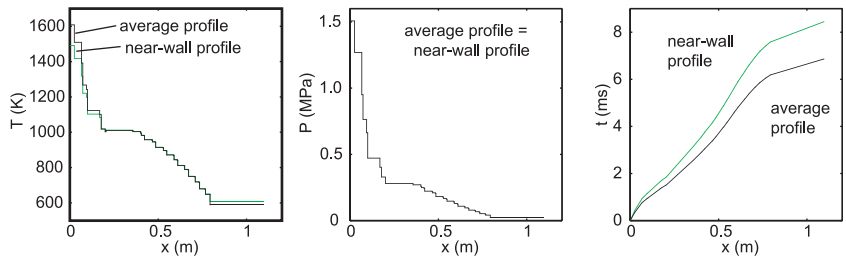

Figure 2. Near-wall and average residence time, temperature, and pressure profiles.

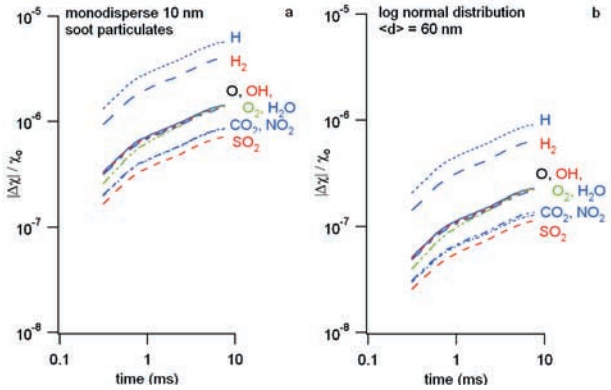

Figure 3. Relative change in gas phase mixing ratio for (a) monodisperse 10 nm diameter soot particulates and (b) a log-normal soot distribution with a mean diameter of 60 nm.

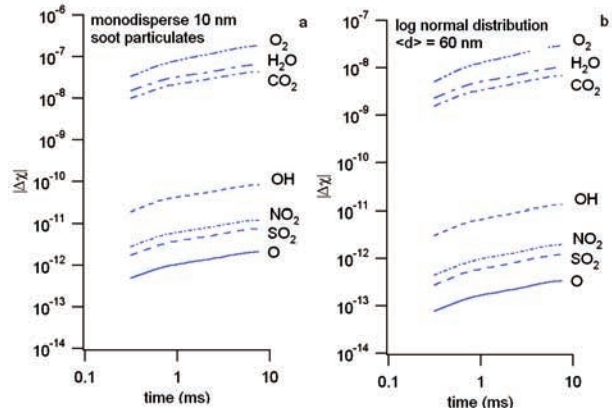

Figure 4. Change in gas phase mixing ratio as a function of time in the turbine for (a) monodisperse 10 nm diameter soot particulates and (b) a log-normal soot distribution with a mean diameter of 60 nm.

eration of the primary 10 nm soot spherules in the combustor flow. In each case the soot emission index is 1.0 g/kg-fuel. This is larger than measured values at the exhaust exit to ensure that the predicted changes due to heterogeneous reactions are upper limits.

[17] A reaction having the global form given by C(s) + X(g) + Y(g) Π products can be neglected if (1) the loss or production of gas phase reactants and (2) the impact of gas phase products on trace speciation through subsequent gas phase reactions are all negligible relative to gas phase chemistry alone. An estimate for the upper limit to these changes is given by (assuming [X]<[Y] where [X] and [Y] are the initial gas phase reactant concentrations)

$$\frac{d[X]}{dt} = \Sigma k_i N_i [X] \tag{1}$$

where N_i is the number density of particles with radius r_i and k_i is the rate per particle given by

$$k_i = \frac{4\pi r_i^2 D}{\frac{4D}{v\alpha} + \frac{r_i^2}{r_i + \lambda}} \tag{2}$$

where D, ν, and λ are the gas phase diffusion coefficient, mean speed, and mean free path, respectively, for the gas phase reactant *X(g)* and α is the reactive uptake probability. Thus, the specific elementary reaction mechanism and any reactive site dependence are ignored. Moreover, α has been set to unity even though room temperature values of α for species like SO_2 and NO_2 interactions with soot and soot like substances are typically of the order 10^{-7}–10^{-4} [*DeMore et al.*, 1994]. Thus, the actual rates are well below those used here.

[18] Figure 3 shows the change in the mixing ratio, $\Delta\chi$, versus time in the turbine relative to the initial mixing ratio at the turbine inlet, χo, for a number of trace species of interest. Figure 3a shows results for monodisperse 10 nm diameter soot particulates. Figure 3b shows results for the log-normal soot distribution given above. The computed relative changes are typically <0.001% for both distributions. The relative changes for the monodisperse distribution are approximately a factor 10 larger than for the log-normal distribution, with NO_2 exhibiting the largest change. However, even in the latter case, $|\Delta\chi|/\chi o$ is less than 0.01% at the exhaust exit. Thus, heterogeneous reactions on soot would have a negligible impact on the direct loss of gas phase reactants even if a larger surface area were available due to the monodisperse distribution.

[19] Figure 4 shows absolute changes in gas phase mixing ratios for the two soot distributions. These results limit the maximum increase in trace speciation that could result from heterogeneous reactions on soot in the turbine. Specifically, $\Delta\chi_p < n_r\ |\Delta\chi_r|$, where $|\Delta\chi_r|$ is the absolute change in the smallest concentration reactant in Equation 1, nr is the product stoichiometric coefficient, and $\Delta\chi_p$ is the change in any of the potential products. From Figure 4 and for nr = 1, $\Delta\chi_p < |\Delta\chi_r| < 10^{-10}$ for all reactants excluding the major combustor exit species O_2, CO_2, and H_2O. Since the $|\Delta\chi_r|/\chi o < 0.01\%$ (Figure 4), the mixing ratio is approximately constant and $|\Delta\chi_r|$ is proportional to χ_o. Thus, four orders-of-magnitude increase in mixing ratios of minor combustion products would be required to achieve $|\Delta\chi_r|$ levels of one ppmv. For O_2, CO_2, and H_2O, $\Delta\chi_p < \Delta\chi_r < 10^{-6}$ indicating a maximum change of 1 ppmv in the mixing ratios for the products of the reactions involving these species.

4. Heterogeneous Reactions on Engine Surfaces

[20] Model results for the absolute change, $|\Delta\chi|$, in the mixing ratios of selected gas phase reactants due to interaction with internal engine surfaces are summarized in Figure 5. The $|\Delta\chi|$ as a function of time is shown for the maximum residence time. In each case the time dependent change in gas phase reactant due

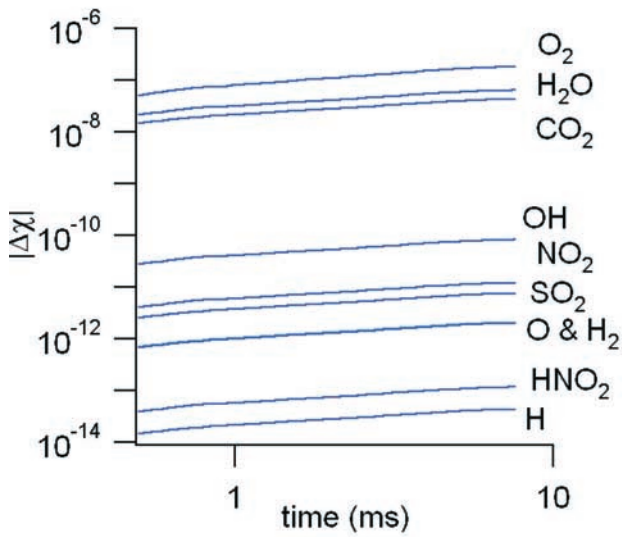

Figure 5. Change in gas phase mixing ratio as a function of time for (a) minimum residence time profiles and (b) maximum residence time profiles.

heterogeneous reactions on internal engine surfaces has been expressed as

$$\frac{d[X]}{dt} = s\left(\frac{\nu_T/4}{e}\right)[X] \tag{3}$$

where the [X] is the concentration of the gas preactant, ν_T is the mean thermal speed multiplied by an adjustment factor of 100 to account for turbulence, e is the near-wall layer extent, and s is the heterogeneous reaction probability (taken to be unity).

[21] Comparing Figures 4 and 5, it can be seen that the estimated changes in species mixing ratios are typically smaller for the heterogeneous reactions on internal engine surfaces than for reactions with combustion soot particulates. While the available surface area for internal surfaces is significantly larger than that available from combustion soot particulates, and the estimated residence time for gas in the boundary layer is longer than the residence time for the core flow (Figure 2), the molecules in the boundary layer that come into contact with the wall surface are only a small percent of the overall flow through the turbine.

5. Summary

[22] The potential impact of heterogeneous reactions on trace species emissions from gas turbine engines was evaluated using a one-dimensional model for the turbine flow of a representative advanced subsonic engine and upper limit approximations to the heterogeneous reaction rates. The analysis considered reactions on combustion soot particulates and post-combustor internal turbine surfaces. For the former, results were presented for monodisperse 10 nm diameter particles and a log-normal distribution that is typical of soot distributions measured near the exhaust exit and in the of currently operational aircraft. In each case, the carbon mass emission index was set to 1.0 g/kg-fuel, which is well above measured values. For heterogeneous reactions on internal engine surfaces, upper limits for the surface area and residence times were determined based on available turbine geometries and time scales for the fluid dynamics in boundary layers.

[23] The results indicate that heterogeneous reactions directly involving trace species as reactants are negligible. This was found to be the case for reactions on turbine surfaces and reactions with combustion soot particulates. Thus, heterogeneous chemistry within the engine cannot explain the high conversion of SO_2 to S(VI) (SO_3, H_2SO_4) that some plume/wake aerosol models require to produce observed levels of volatile (presumably sulfuric acid) aerosols. Also, internal engine heterogeneous processes will also have no significant effect on exhaust NO_x or NO_y levels.

[24] **Acknowledgments.** We would like to thank the NASA Atmospheric Effects of Aviation Project for funding and logistical support, Dr. Chowen Wey of the NASA Lewis Research Center for material support and guidance, and Tony Chobot and Kerem Limon of the MIT Aero-Environmental Laboratory for their assistance in organizing materials for this study. The authors would also like to thank Dr. Charles E. Kolb for helpful comments.

References

Brideman, M. J., D. G. Cherry, and J. Pederson, Low Pressure Turbine Scaled Test Vehicle Performance Report, NASA CR-168290, 1983.

DeMore, W. B., et al., Chemical kinetics and photochemical data for use in stratospheric modeling, Evaluation II, JPL, Publ. 94-26, Jet Propul. Lab. Pasadena, CA., Aug., 1994.

Friedrichs, S., H. P. Hodson, and W. N. Dawes, Aerodynamic Aspects of Endwall Film-Cooling, *Journal of Turbomachinery*, *119*, 786–793, October 1997.

Grobman, J. S., Effect of operating variables on pollutant emissions from aircraft turbine engine combustors, in Emissions from Continuous Combustion Systems, Proceedings of the Symposium on Emissions from Continuous Combustion Systems, edited by W. Cornelius and W. G. Agnew, Plenum Press, 1972.

Harasgama, S. P., Combustor Exit Temperature Distortion Effects on Heat Transfer and Aoerdynamics within a Rotating Turbine Blade Passage, ASME 90-GT-174, 1990.

Hall, E. J., S. R. Lynn, N. J. Heidegger, and R. A. Delaney, Energy Efficient Engine Low Pressure Subsystem Flow Analysis, NASA CR-1998-206597, April 1998.

Howard, R. P., R. S. Hiers, P. D. Whitefield, D. E. Hagen, J. C. Wormhoudt, R. C. Miake-Lye, and R. Strange, Experimental characterization of gas turbine emissions at simulated flight altitude conditions, Technical Report AEDC-TR-96-3, Arnold Engineering Development Center, Arnold Air Force Base, TN., 1996.

Kang, S., F. Lin, and Z. Wang, A Method for Calculating Axial Turbomachinery End Wall Turbulent Boundary Layers, ASME 89-GT-15, 1989.

Klebanoff, P. S., Characteristics of Turbulence in a Boundary Layer with Zero Pressure Gradient, NASA Report 1247, 1955.

Knight, C. J., and D. Choi, Development of a Viscous Cascade Code Based on Scalar Implicit Factorization, AIAA Journal, *27*(5), 81, 1989.

Kuethe, A. M., and C.-Y. Chow, Foundations of Aerodynamics-Bases of Aerodynamic Design, Fourth Edition, New York: John Wiley and Sons, 1986.

Lakshiminarayama, B., Fluid Dynamics and Heat Transfer of Turbomachinery, New York: John Wiley and Sons, Inc., 1996.

Lakshiminarayama, B., and T. R. Govindar, Analysis of Turbulent Boundary Layer on Cascade and Rotor Blades of Turbomachinery, AIAA Journal, *19*, 1333–1341, 1981.

Leach, K. P., Energy Efficient Engine-High Pressure Turbine component Rig Performance Test, NASA CR-168189, 1983.

Liebeck, R. H., D. A. Andrastek, J. Chau, R. Girvin, R. Lyon, B. K. Rawdon, P. W. Scott, and R. A. Wright, Advanced subsonic design and economic studies, NASA CR-195443, April, 1995.

Lukachko, S. P., Research on the science and politics of the atmospheric effects of aviation debate, S.M. thesis, Massachusettes Institute of Technology, Cambridge, 1997.

Lukachko, S. P., I. A. Waitz, R. C. Miake-Lye, R. C. Brown, and M. R. Anderson, Production of sulfate aerosol precursors in the turbine and exhaust nozzle of an aircraft engine, *J. Geophys. Res.*, *103*, 16159–16174, 1998.

Lyon, T. F., and D. W. Bahr, CF6-50 Engine Emissions Testing with Traverse Probe, Final Report, FAA-CT-81-18, 1981.

Moss, R. W., and M. L. G. Oldfield, Measurements of the Effect of Free-Stream Turbulence Length Scale on Heat Transfer, Presented at the International Gas Turbine and Aeroengine Congress and Exposition, Cologne, Germany, June 1–4, 1992.

Petzold, A., and F. P. Schroder, Jet Engine Exhaust Aerosol Measurement, *Aero. Sci. Tech.*, *28*, 62–76, 1998.

Schlichting, H., Boundary Layer Theory, Seventh Edition, New York:McGraw-Hill, 1979.

Shang, T., Influence of Inlet Temperature Distortion on Turbine Heat Transfer, Ph.D. Thesis. Massachusetts Institute of Technology, 1995.

Sharma, O. P., E. Renaud, T. L. Butler, K. Milsaps Jr., R. P. Gring, and H. D. Joslyn, Rotor-Stator Interaction in Multi-Stage Axial-Flow Turbines, AIAA-88-3010, July 1998.

Zeschky, J., and H. E. Gallus, Effects of Stator Wakes and Spanwise Nonuniform Inlet Conditions on the Rotor Flow of an Axial Turbine Stage, ASME 91-GT-93, 1991.

R. C. Brown and R. C. Miake-Lye, Aerodyne Research, Inc., 45 Manning Road, Billerica, MA.

S. P. Lukachko and I. A. Waitz, Massachusetts Institute of Technology, Cambridge, MA.